

3) the corrected values for the transition energies in keV. The uncertainties in the values of  $E_{th}$  in Table II range from 5 to 10 eV, and are the same as in Dixit *et al.* We see now by a comparison of the theoretical and experimental values that the discrepancy is reduced considerably, the only transitions having any significant discrepancy being the  $4f-3d$  transition in Ba and the  $5g-4f$  transition in Pb.

We have also considered the effect of the finite size of the nucleus on the vacuum-polarization corrections: The rather complicated convolution integral required to do this in configuration space becomes a trivial multiplicative factor in the momentum-space integral. Taking the uniform model for the nuclear shape, we find that the individual shifts are increased by rather less than 1%, giving less than 10 eV from the Uehling term itself, and correspondingly smaller corrections from the higher-order terms. A more realistic model for the nuclear shape can hardly be expected to give rise to any significant difference.

An effect of the same magnitude arises if the vacuum-polarization potential is included in the Dirac equation itself, rather than treating it perturbatively as we have done. The  $E_{th}$  in Table II is, in fact, calculated by the former method; the difference between this value and the perturbative value is of the order of 10 eV.

A number of authors<sup>5,6</sup> have suggested a possible anomalous interaction of the muon via a scalar field. The model suggested by Barshay,<sup>5</sup> with a scalar meson of mass around 750 MeV, turns out to give shifts of less than 1 eV for the states in which our interest lies; this is because the large mass implies a very short-range force

which dominantly affects only the S-wave states. We note that the  $4f-3d$  transition in Ba and the  $5g-4f$  transition in Pb have almost equal discrepancies of about 70 eV. This enables us to put a rather good upper limit on the mass  $m_s$  of the scalar meson of about 8 MeV. Assuming this mass, the required coupling constant is  $G_s = g_s \mu \mu \times g_{sNN} = 6 \times 10^{-7}$ . The final column in Table II shows the theoretical value, including the effects of this particle, once again incorporating the effects of the finite nuclear size. It is remarkable that the remaining discrepancy is eliminated: The reader is at liberty to regard this as evidence for a physical particle of mass 8 MeV, coupling mainly to  $\mu^+ \mu^-$ . It is amusing to speculate that if this particle is very weakly coupled to  $e^+ e^-$ , it would escape experimental detection, as well as provide a mechanism for the breaking of  $\mu e$  universality.

The authors would like to thank Professor E. P. Hincks, Professor D. Kessler, and Professor H. L. Anderson for discussions.

---

\*Work supported in part by the National Research Council of Canada.

<sup>1</sup>M. S. Dixit, H. L. Anderson, C. K. Hargrove, R. J. McKee, D. Kessler, H. Mes, and A. C. Thompson, *Phys. Rev. Lett.* **27**, 878 (1971).

<sup>2</sup>B. Fricke, *Z. Phys.* **218**, 495 (1969).

<sup>3</sup>G. Kallen and A. Sabry, *Kgl. Dan. Vidensk. Selsk., Mat.-Fys. Medd.* **29**, No. 17 (1955).

<sup>4</sup>E. Wichmann and N. M. Kroll, *Phys. Rev.* **101**, 843 (1956).

<sup>5</sup>S. Barshay, *Phys. Lett.* **37B**, 397 (1971).

<sup>6</sup>S. Weinberg, *Phys. Rev. Lett.* **27**, 688 (1971).

---

## EPR Investigations of $Ce^{3+}$ in Cubic Sites of CaO, SrO, and BaO<sup>†</sup>

R. W. Reynolds,\* Y. Chen, L. A. Boatner,\* and M. M. Abraham

*Solid State Division, Oak Ridge National Laboratory, Oak Ridge, Tennessee 37830*

(Received 17 April 1972)

The EPR of  $Ce^{3+}$  has been observed in sites of cubic symmetry for the first time. The unusually large deviation of the observed  $g$  values for  $Ce^{3+}$  in CaO, SrO, and BaO from the theoretical value calculated for a pure  $\Gamma_7$  ground state can be attributed mainly to static crystal-field admixtures.

The electron paramagnetic resonance (EPR) spectrum of  $Ce^{3+}$  ( $4f^1$  configuration) in cubic single crystals has previously been the subject of numerous investigations.<sup>1-6</sup> Until the present

work, however, no EPR spectra have been reported which could be attributed unequivocally to  $Ce^{3+}$  in a cubic symmetry site.<sup>7</sup> The observation of the EPR spectrum of  $Ce^{3+}$  in a site of local cu-

bic symmetry is of special interest, first, because of the sizable discrepancy previously found to exist between the observed and calculated  $g$  values for  $Ce^{3+}$  in lower symmetry sites; and, second, because the simplicity of the electronic configuration and cubic symmetry make the system a facile case for calculations of the mechanisms for producing  $g$ -value variations.

In particular, observation of the  $Ce^{3+}$  cubic-site  $g$ -value variations in a series of isomorphous host materials such as CaO, SrO, and BaO should serve to distinguish between the following three mechanisms previously proposed to explain the discrepancies: (1) admixture of excited states into the  $Ce^{3+}$  ground state by the static crystal-line electric field of the host; (2) similar admixture by the orbit-lattice interaction (i.e., a dynamic crystal-field admixture); and (3) reduction of the ground-state orbital angular momentum by covalent bonding.

We report here the successful production of  $Ce^{3+}$  ions in cubic symmetry sites in CaO and SrO single crystals and BaO powder. The observed  $g$  values were found to differ considerably from those calculated for the expected pure ground state of  $Ce^{3+}$  in these hosts.<sup>8</sup> From the size of this deviation, it is likely that most of the variation can be attributed to static crystal-field admixtures.

Single crystals of  $Ce^{3+}$ -doped CaO, SrO, and MgO were grown by an arc-fusion process described previously.<sup>9</sup> Polycrystalline samples of  $Ce^{3+}$ -doped BaO were also obtained by the same technique. Chemical analyses verified the presence of Ce in all four hosts. These crystals have the NaCl, rock-salt structure, and  $Ce^{3+}$  ions located in cation substitutional sites would have sixfold cubic (octahedral) coordination. The  $Ce^{3+}$  free ion has a  ${}^2F_{5/2}$  ground state which is separated from the next excited  ${}^2F_{7/2}$  state by  $\approx 2250$   $cm^{-1}$ . The next free-ion level is of the order of

50 000  $cm^{-1}$  higher. In a cubic crystal field, the  ${}^2F_{5/2}$  level splits into a  $\Gamma_7$  doublet and a  $\Gamma_8$  quartet, with the  $\Gamma_7$  lowest in sixfold coordination. EPR transitions within the pure  $\Gamma_7$  doublet should have an isotropic  $g$  value of  $-\frac{10}{7}$ .

The X-band EPR spectra observed for  $Ce^{3+}$  in CaO, SrO, and BaO consisted of a single isotropic line, which was seen at temperatures up to  $\approx 100$  K for CaO and SrO. This detection of the EPR spectra of  $Ce^{3+}$  at such elevated temperatures is very unusual for a non-S-state rare-earth ion. Temperatures below 77 K were required for observation of the  $Ce^{3+}$  spectrum in BaO. No resonance signals were observed for Ce-doped MgO, although as noted previously, Ce was detected by spectroscopic analysis. It is believed that Ce was not incorporated in MgO in the trivalent state. Lower-symmetry EPR spectra due to  $Ce^{3+}$  were also detected in CaO and SrO, but their low intensity and small  $g$  values made the analysis difficult. In the single-crystal samples, the cubic-site EPR linewidth varied with magnetic field orientation, being narrowest ( $\approx 7$  G at 4.2 K) with  $\vec{H} \parallel [100]$  and broadest ( $\approx 50$  G at 4.2 K) with  $\vec{H} \parallel [111]$ . This linewidth variation is exactly opposite to that found for  $Co^{2+}$  and  $Fe^{1+}$  and for the rare-earth ions  $Dy^{3+}$ ,  $Tm^{2+}$ , and  $Yb^{3+}$  in the oxides where the narrowest lines occurred for  $\vec{H} \parallel [111]$ .<sup>8,10,11</sup>

The observed cubic-site  $g$  values are given in column 1 of Table I. It is obvious from this table that the  $g$  values differ considerably from each other and from the expected absolute value of  $\frac{10}{7}$ . In the absence of measured crystal-field strengths for these crystals, it is impossible to identify positively the cause of these deviations. However, the large magnitude of the deviation from  $|g| = \frac{10}{7}$  tends to eliminate the orbit-lattice interaction and covalent bonding as the dominant processes. Birgeneau<sup>12</sup> has shown for  $Ce^{3+}$  in rare-earth ethylsulfates that much of the reduction of

TABLE I.  $Ce^{3+}$  EPR and crystal-field parameters for CaO, SrO, and BaO.

	$ g $	$\varphi$ (deg)	Point-charge model		Alternate model	
			$B_0^{(6)}/B_0^{(4)}$	$B_0^{(4)}$ ( $cm^{-1}$ )	$B_0^{(6)}/B_0^{(4)}$	$B_0^{(4)}$ ( $cm^{-1}$ )
CaO	$0.7963 \pm 0.0003$	14.63	0.066	4 950	0.1	5 750
		29.83		13 100		15 210
SrO	$0.8948 \pm 0.0005$	12.98	0.057	4 200	0.1	5 050
		28.28		11 400		13 700
BaO	$0.9340 \pm 0.0007$	12.29	0.050	3 850	0.1	4 760
		27.49		10 600		13 130

the observed  $g$  values from the calculated values can be explained by the simultaneous action of the Zeeman and orbit-lattice interactions. In this fashion he was able to explain reductions of the  $g$  values of the order of  $\approx 10\%$ . Similarly, Inoue,<sup>13</sup> who first suggested the orbit-lattice interaction as a cause of  $g$ -value variations, found this mechanism to cause a deviation of 0.1% in the  $g$  value of  $\text{Tm}^{2+}$  in  $\text{CaF}_2$  and 1.7% in the  $g$  value of  $\text{Ho}^{2+}$  in  $\text{CaF}_2$ . However, for  $\text{Ce}^{3+}$  in the oxides, our observed deviation of  $g$  from the calculated value is much larger (35–44%) and, thus, it is not likely that the orbit-lattice interactions is the dominant mechanism. The effect of covalent bonding on the observed  $g$  value is frequently expressed by means of an orbital reduction factor  $k$ . For the specific case of the  $\Gamma_7$  ground state of  $\text{Ce}^{3+}$ , the  $g$  value varies with  $k$  as

$$g = -\frac{10}{7} + \frac{40}{21}(1-k). \quad (1)$$

A value of  $1-k$  in the range 0.26–0.33 is required to explain our observed  $g$  values in the oxides. Such values of  $1-k$  are 2 orders of magnitude larger than those calculated for  $\text{Tm}^{2+}$  in  $\text{CaF}_2$ <sup>14</sup> and almost 1 order of magnitude greater than that proposed to explain the EPR spectrum of

$\text{Yb}^{3+}$  in  $\text{CaO}$ .<sup>15</sup> Covalent bonding, therefore, cannot be considered as the dominant factor in the  $g$ -value variations of  $\text{Ce}^{3+}$  in the oxides. It should be emphasized, however, that the corrections produced by these two mechanisms (covalency and orbit-lattice interactions) are in the right direction (i.e., towards smaller  $g$  values).

In contrast to the complexity of the preceding two mechanisms, it is relatively easy to calculate the value of the static crystalline electric field necessary to explain the observed  $g$  values. A cubic crystal field of moderate strength will admix the ground  $\Gamma_7$  doublet with the  $\Gamma_7$  doublet of the next excited  ${}^2F_{7/2}$  manifold. The resulting state will have the form

$$|\pm\rangle = \cos\varphi |J=\frac{5}{2}, \Gamma_7^\pm\rangle - \sin\varphi |J=\frac{7}{2}, \Gamma_7^\pm\rangle, \quad (2)$$

where

$$\begin{aligned} |J=\frac{5}{2}, \Gamma_7^\pm\rangle &= (\frac{1}{6})^{1/2} |\pm\frac{5}{2}\rangle - (\frac{5}{6})^{1/2} |\mp\frac{3}{2}\rangle, \\ |J=\frac{7}{2}, \Gamma_7^\pm\rangle &= -\frac{1}{2}\sqrt{3} |\pm\frac{5}{2}\rangle + \frac{1}{2} |\mp\frac{3}{2}\rangle, \end{aligned}$$

and  $\varphi$  represents the degree of admixture. The  $\Gamma_7$  states shown above are given in terms of  $|\pm M_J\rangle$  basis states. The ground-state  $g$  value is given by

$$g = 2\langle + | L_z + 2S_z | + \rangle = -\frac{10}{7} \cos^2\varphi + \frac{16}{21}\sqrt{3} \sin\varphi \cos\varphi + \frac{24}{7} \sin^2\varphi, \quad (3)$$

where the pure Russell-Saunders coupling values have been used for the Landé  $g$  factors. With the assumption that the measured  $g$  values are negative, Eq. (3) can be solved to give two possible values of  $\varphi$  for each measured  $g$  value. These values of  $\varphi$  are listed in column 2 of Table I. Although it is impossible on the basis of the  $g$  value alone to distinguish between the two values of  $\varphi$ , they can be related to the cubic-crystal-field parameters. The cubic-crystal-field Hamiltonian is given by the expression<sup>16</sup>

$$V_c = B_0^{(4)} [C_0^{(4)} + (\frac{5}{14})^{1/2} (C_{-4}^{(4)} + C_{+4}^{(4)})] + B_0^{(6)} [C_0^{(6)} - (\frac{7}{2})^{1/2} (C_{-4}^{(6)} + C_{+4}^{(6)})] \quad (4)$$

[written here in the form usually employed in the tensor-operator approach to crystal-field theory, where  $C_q^{(k)} = 2(2k+1)^{-1/2} Y_k^q$  with  $Y_k^q$  the appropriate spherical harmonic function]. It can then be shown that

$$\tan 2\varphi = \frac{2\langle J=\frac{5}{2}, \Gamma_7 | V_c | J=\frac{7}{2}, \Gamma_7 \rangle}{E_{s.o.} + \langle J=\frac{7}{2}, \Gamma_7 | V_c | J=\frac{7}{2}, \Gamma_7 \rangle - \langle J=\frac{5}{2}, \Gamma_7 | V_c | J=\frac{5}{2}, \Gamma_7 \rangle}, \quad (5)$$

where  $E_{s.o.}$  is the splitting of the levels produced by the spin-orbit interaction ( $\approx 2250 \text{ cm}^{-1}$ ). Upon evaluation of the matrix elements, Eq. (5) becomes a relation between  $\varphi$  and the crystal-field parameters  $B_0^{(4)}$  and  $B_0^{(6)}$ . At this point some relationship between  $B_0^{(4)}$  and  $B_0^{(6)}$  must be assumed. The point-charge model, considering only nearest-neighbor ions, can be used to give a rough estimate of the ratio of  $B_0^{(6)}$  to  $B_0^{(4)}$ .

Explicitly, the relation is

$$\frac{B_0^{(6)}}{B_0^{(4)}} = \frac{3}{14R^2} \frac{\langle r^6 \rangle}{\langle r^4 \rangle}, \quad (6)$$

where the  $R$  is the separation between the impurity and the coordinating ions, and  $\langle r^n \rangle$  is the mean  $n$ th power of the  $4f$  electron radius.<sup>17</sup> If the values of Wakim *et al.*<sup>18</sup> for  $\langle r^n \rangle$  and the value of  $R$

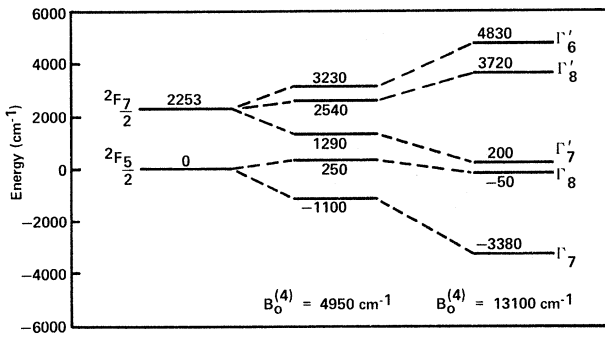


FIG. 1. Energy levels of  $\text{Ce}^{3+}$  in  $\text{CaO}$ . The simple point-charge model predicts a ratio of  $B_0^{(6)}/B_0^{(4)} = 0.066$ . With this assumption the energy levels are shown for the two possible choices for  $B_0^{(4)}$ .

appropriate to the unperturbed crystal lattice are substituted in Eq. (6), the  $B_0^{(6)}/B_0^{(4)}$  values shown in column 3 of Table I result. This relation and Eq. (5) can then be used to solve for  $B_0^{(4)}$  and  $B_0^{(6)}$ . The value of  $B_0^{(4)}$  resulting from each value of  $\varphi$  is shown in column 4 of Table I. A better value of  $B_0^{(6)}/B_0^{(4)}$  is probably that obtained from experimental determinations of this quantity for other rare-earth ions in the oxides. For  $\text{Er}^{3+}$  in  $\text{MgO}$ ,  $\text{CaO}$ , and  $\text{SrO}$  and for  $\text{Nd}^{3+}$  in  $\text{CaO}$ ,<sup>19-21</sup> the experimentally determined ratio  $B_0^{(6)}/B_0^{(4)}$  is larger than that computed from the simple point-charge model by a factor of approximately 1.5–2.0. Therefore, a ratio of  $B_0^{(6)}/B_0^{(4)} = 0.1$  is probably a more accurate estimate for all the oxide hosts. The values of  $B_0^{(4)}$  resulting from the latter ratio are shown in the last column of Table I (i.e., the alternate model). For either value of  $\varphi$ , the crystal-field splittings computed from these parameters are anomalously

TABLE II. Observed crystal-field splitting for the  ${}^2F_{5/2}$  and  ${}^2F_{7/2}$  states of  $\text{Ce}^{3+}$  in various host crystals.

	$J = \frac{5}{2}$ ( $\text{cm}^{-1}$ )	$J = \frac{7}{2}$ ( $\text{cm}^{-1}$ )
$\text{LaCl}_3^a$	110.0	233.5
$\text{LaF}_3^b$	...	684.5
$\text{CeF}_3^b$	...	690
$\text{CeES}^c$	94.5	...
$\text{YGaG}^d$	402	1509

<sup>a</sup>K. H. Hellwege, E. Orlich, and G. Schaack, *Phys. Kondens. Mater.* **4**, 196 (1965).

<sup>b</sup>R. A. Buchanan, H. E. Rast, and H. H. Caspers, *J. Chem. Phys.* **44**, 4063 (1966).

<sup>c</sup>Birgeneau, Ref. 12.

<sup>d</sup>G. F. Herrman, J. J. Pearson, K. A. Wickersheim, and R. A. Buchanan, *J. Appl. Phys.* **37**, 1312 (1966).

ly large. Figure 1 shows the computed splittings of  $\text{Ce}^{3+}$  in  $\text{CaO}$  using both choices of  $B_0^{(4)}$  and the  $B_0^{(6)}/B_0^{(4)}$  ratio given by the point-charge model. The splittings calculated for each  $J$  manifold can be compared to the splittings observed previously in other hosts and given in Table II. From inspection of Table II it is clear that the smaller value of  $B_0^{(4)}$  shown in Fig. 1 is the more likely of the two choices for  $\text{CaO}$  and, hence, is probably the more acceptable choice for all three hosts. However, even the smaller values of  $B_0^{(4)}$  represent large splittings, and not all of the  $g$ -value variation may result from static crystal-field effects. A combination of all three of the mechanisms previously noted represents the most likely explanation for our results.

†Research sponsored by the U. S. Atomic Energy Commission under contract with Union Carbide Corporation.

\*Advanced Technology Center, Inc., Dallas, Tex.

<sup>1</sup>J. M. Baker, W. Hayes, and D. A. Jones, *Proc. Phys. Soc., London* **73**, 942 (1959).

<sup>2</sup>M. Dvir and W. Low, *Proc. Phys. Soc., London* **75**, 136 (1960).

<sup>3</sup>M. J. Weber and R. W. Bierig, *Phys. Rev.* **134**, A1492 (1964).

<sup>4</sup>S. D. McLaughlan and P. A. Forrester, *Phys. Rev.* **151**, 311 (1966).

<sup>5</sup>A. A. Antipin, I. N. Kurkin, G. K. Chirkin, and L. Ya. Shekun, *Fiz. Tverd. Tela* **6**, 2014 (1965) [*Sov. Phys. Solid State* **6**, 1590 (1965)].

<sup>6</sup>A. Kafri, D. Kiro, S. Yatsiv, and W. Low, *Solid State Commun.* **6**, 573 (1968); D. Kiro, W. Low, and D. Kafri, *Phys. Rev. Lett.* **22**, 893 (1969); D. Kiro and W. Low, *Phys. Lett.* **29A**, 537 (1969).

<sup>7</sup>It should be pointed out that the EPR spectrum of  $\text{Pa}^{4+}$  ( $5f^1$  configuration) has been reported for pure octahedral symmetry (i.e., a  $\text{Cs}_2\text{ArCl}_6$  host). J. D. Axe, H. J. Stapleton, and C. D. Jeffries, *Phys. Rev.* **121**, 1630 (1960). Subsequent investigations, however [C. D. Jeffries and H. J. Stapleton, reported in J. D. Axe, Lawrence Radiation Laboratory Report No. UCLRL-9293, (unpublished)] have shown an anisotropy in the  $\text{Pa}^{4+}$  spectrum. This anisotropy was attributed to a distortion of the local crystal field.

<sup>8</sup>R. W. Reynolds, M. M. Abraham, L. A. Boatner, and Y. Chen, *Bull. Amer. Phys. Soc.* **16**, 360 (1971).

<sup>9</sup>M. M. Abraham, C. T. Butler, and Y. Chen, *J. Chem. Phys.* **55**, 3752 (1971).

<sup>10</sup>See the review by W. Low and E. L. Offenbacher, in *Solid State Physics*, edited by H. Ehrenreich, F. Seitz, and D. Turnbull (Academic, New York, 1965), Vol. 17, p. 135.

<sup>11</sup>M. M. Abraham, R. W. Reynolds, and L. A. Boatner, *Phys. Rev.* **175**, 485 (1968); R. W. Reynolds, Ph. D. thesis, Vanderbilt University, Nashville, Tennessee,

1969 (unpublished).

<sup>12</sup>R. J. Birgeneau, Phys. Rev. Lett. **19**, 160 (1967).

<sup>13</sup>M. Inoue, Phys. Rev. Lett. **11**, 196 (1963), and Ph. D. thesis, Harvard University, Cambridge, Massachusetts, 1963 (unpublished).

<sup>14</sup>B. Bleaney, Proc. Roy. Soc., Ser. A **277**, 289 (1964).

<sup>15</sup>W. Low and R. S. Rubins, Phys. Rev. **131**, 2527 (1963).

<sup>16</sup>B. G. Wybourne, *Spectroscopic Properties of Rare Earths* (Interscience, New York, 1965).

<sup>17</sup>K. R. Lea, M. J. M. Leask, and W. P. Wolf, J.

Phys. Chem. Solids **23**, 1381 (1962).

<sup>18</sup>F. G. Wakim, M. Synek, P. Grossgut, and A. Dammomio, Phys. Rev. A **5**, 1121 (1972).

<sup>19</sup>I. C. Chang, Stanford Electronics Laboratories, Stanford, California, Technical Report No. 0174-1, 1965 (unpublished); I. C. Chang and W. W. Anderson, Phys. Lett. **13**, 112 (1964).

<sup>20</sup>D. Deschamps and Y. Merle D'Aubign e, Phys. Lett. **8**, 5 (1964).

<sup>21</sup>A. Wasieleski and Y. Merle D'Aubign e, Phys. Status Solidi (b) **47**, 663 (1971).

## Positron Annihilation in Metals\*

P. Bhattacharyya and K. S. Singwi

Physics Department, Northwestern University, Evanston, Illinois 60201

(Received 6 March 1972)

We derive a nonlinear integral equation, which has three-body correlations built in it, for the Fourier transform of the polarization charge around a positron in an electron liquid. The calculated annihilation rate of the positron in the entire metallic density range, besides being in very good agreement with experiment, merges smoothly into the mean positronium lifetime for larger density. To illustrate the large nonlinear effects, the polarization charge around a fixed proton for a density  $r_s=2$  has also been calculated.

The first successful theory of positron annihilation in metals with density  $r_s \leq 4$  is due to Kahana,<sup>1</sup> who realized the importance of nonlinearity and used the "ladder" approximation to treat

the problem. Although the theory was later improved upon by Carbotte,<sup>2</sup> there was no essential difference between the two theories as regards the values of annihilation rates  $\lambda$ . Later Crowell,

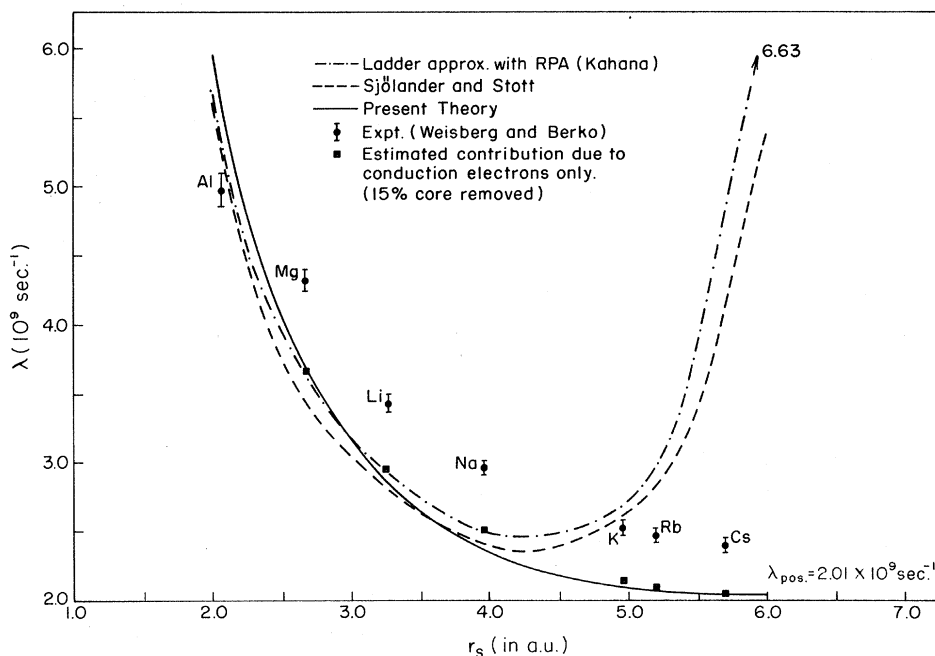


FIG. 1. Positron annihilation rate  $\lambda$  versus  $r_s$  calculated from Eq. (5); other theoretical results of Kahana (Ref. 1) as calculated by Crowell, Anderson, and Ritchie (Ref. 3) and Sj lander and Stott (Ref. 5) and the experimental results of Weisberg and Berko (Ref. 4).